

Z_2 spin liquid phase on the kagome lattice: a new saddle point

Tao Li

Department of Physics, Renmin University of China, Beijing 100872, P.R.China

(Dated: November 7, 2018)

We have performed large scale variational search for the best RVB ansatz for the spin- $\frac{1}{2}$ kagome antiferromagnet with both nearest-neighbor(NN) and next-nearest-neighbor(NNN) exchanges assuming only translational symmetry. We find the best RVB state is always fully symmetric and has a mean field ansatz that is gauge equivalent to a previous proposed Z_2 spin liquid ansatz. The Z_2 state is found to be slightly more stable than the extensively studied U(1) gapless Dirac spin liquid state in both the $J_2 \neq 0$ and the $J_2 = 0$ case and to possess a small spinon gap for $J_2 < 0.2$. The breaking of the U(1) gauge symmetry in the Z_2 state is found to increase with J_2 and to be quite substantial around $J_2 = 0.15$. However, we find the Z_2 state is always very close to the gapless U(1) Dirac spin liquid state, although they have very different RVB parameters. We argue the kagome antiferromagnet should be better understood as a near critical system, rather than a system deep inside a gapped spin liquid phase with well established Z_2 topological order.

PACS numbers:

The search for spin liquid state in frustrated quantum antiferromagnets has attracted a lot of attention in the strongly correlated electron system community. The spin- $\frac{1}{2}$ kagome antiferromagnet is a particularly promising system for this purpose because of the strong geometrical frustration and the low coordinate number of the lattice. Early studies on small clusters find the ground state of the kagome antiferromagnet with NN exchange has no signature of any symmetry breaking and is very likely a quantum spin liquid¹⁻⁸. However, the exact nature of such a spin liquid phase is still under intense debate^{9,10}. Especially, it is found that the gap for triplet excitation above the ground state is very small, although the spin correlation length is only of the order of the lattice constant. More curiously, it is found that the spin singlet channel of the system may host an exponentially large number of low energy excitations below the exceptional small spin gap¹¹⁻¹⁴.

The quest for the true nature of the ground state of the kagome antiferromagnet becomes even more urgent after its material realization in the $ZnCu_3(OH)_6Cl_2$ systems¹⁵⁻¹⁷. Recently, extensive DMRG simulations has been performed on the kagome antiferromagnets both with only NN exchange and that with more extended exchange couplings¹⁸⁻²⁴. The DMRG results seem to indicate that the kagome antiferromagnet with NN exchange has a small but finite gap in both spin triplet and spin singlet channel, which is in support of a gapped Z_2 spin liquid scenario. However, it is found that the $\ln 2$ topological entanglement entropy expected for a gapped Z_2 spin liquid can only be faithfully demonstrated when one introduce a finite NNN exchange coupling²¹. The abundance of low energy singlet excitations in the system¹¹ also raises the suspicion that the DMRG results may not represent the intrinsic property of the system in the thermodynamic limit, since open boundary condition is adopted in all DMRG simulations and symmetry breaking perturbations in the singlet channel can be super relevant.

Another scenario on the spin liquid ground state of the kagome antiferromagnets is provided by variational studies based on the RVB theory. It was found previously that the best RVB state for the ground state of the kagome antiferromagnet with NN exchange coupling is a U(1) spin liquid state with a Dirac-type spinon dispersion^{25,26}. Extensive studies on this state find it is actually a very robust saddle point provided that the symmetry of the system is unbroken²⁷⁻²⁹. Attempts to break the U(1) gauge symmetry (and to introduce spin gap) always result in increase of energy in the thermodynamic limit. More recently, study on the $J_1 - J_2$ Heisenberg model on the kagome lattice has been performed and it is found that the U(1) Dirac spin liquid state remains the most stable phase even when J_2 is quite large³⁰. This is strange since strong evidence for Z_2 topological order has already been reported in DMRG simulation in this case. The U(1) Dirac spin liquid state is thus argued to form a stable phase in the phase diagram around the NN Heisenberg model point, rather than a single quantum critical point.

In this work, we reinvestigate the possible spin liquid ground state of the kagome antiferromagnet with the RVB theory. To reduce bias in our study, we only assume translational symmetry for the RVB state at the beginning. We have performed large scale variational search for the best RVB ground state for the $J_1 - J_2$ model on the kagome lattice with up to the second neighbor RVB order parameters. We find the best RVB state is a fully symmetric spin liquid with a mean field ansatz that is gauge equivalent to a Z_2 ansatz proposed previously from the analysis of projective symmetry group (PSG) on the kagome lattice²⁷. Different from a previous study on the same state, we find a finite spin gap and Z_2 gauge structure can be indeed be stabilized in both the $J_2 \neq 0$ and the $J_2 = 0$ case, although the energy advantage over the U(1) gapless state is very small. We find the extent of U(1) gauge symmetry breaking increases with J_2 . However, the spin gap is found to follow the opposite trend

and vanishes around $J_2 = 0.2$. The size of the spin gap is found to be very small.

The model we study in this paper is given by

$$H = J_1 \sum_{\langle i,j \rangle} S_i \cdot S_j + J_2 \sum_{\langle\langle i,j \rangle\rangle} S_i \cdot S_j \quad (1)$$

The motivation to introduce J_2 is to perturb away the system from the U(1) Dirac spin liquid phase and to stabilize the possible Z_2 spin liquid phase²¹⁻²⁴. Here $\langle i, j \rangle$ denotes NN pair of sites, $\langle\langle i, j \rangle\rangle$ denotes NNN pair of sites. To describe the possible Z_2 spin liquid phase on the kagome lattice, we rewrite the spin operators in terms of the slave particle operators $S = \frac{1}{2} \sum_{\alpha, \beta} f_{\alpha}^{\dagger} \sigma_{\alpha, \beta} f_{\beta}$ and introduce the following mean field ansatz for the slave Fermion f_{α}

$$H_{MF} = \sum_{i,j} \psi_i^{\dagger} U_{i,j} \psi_j \quad (2)$$

in which $\psi_i = (f_{i,\uparrow}, f_{i,\downarrow})$ is the Nambu spinor constructed from the slave Fermion. $U_{i,j} = \begin{pmatrix} \chi_{i,j} & \Delta_{i,j}^* \\ \Delta_{i,j} & -\chi_{i,j}^* \end{pmatrix}$ is a 2×2 matrix with its matrix element $\chi_{i,j}$ and $\Delta_{i,j}$ representing the hopping and pairing type RVB order parameters for the ansatz. The RVB state is constructed by Gutzwiller projection of the mean field ground state and is given by

$$|\text{RVB}\rangle = P_G |\{\chi_{i,j}, \Delta_{i,j}\}\rangle, \quad (3)$$

here $|\{\chi_{i,j}, \Delta_{i,j}\}\rangle$ denotes the mean field ground state of H_{MF} and is a generalized BCS-type state. P_G denotes the Gutzwiller projection to remove the doubly occupied configuration in the mean field ground state. The resultant RVB state can be simulated efficiently with the variational Monte Carlo method.

In our RVB state we will keep RVB order parameters $U_{i,j}$ up to the second neighboring bonds. To represent a fully symmetric spin liquid state, these RVB order parameters should be invariant under the symmetry operations of the Hamiltonian up to some SU(2) gauge transformations of the form $U_{i,j} \rightarrow G_i U_{i,j} G_j^{\dagger}$. Here G_i is a SU(2) matrix acting on the Nambu spinor ψ_i . The symmetric RVB state so constructed can be classified into distinct PSGs according to the gauge transformations $\{G_i\}$ needed to restore the form of the RVB order parameters after the symmetry operations. Here we will only assume the translational symmetry at the beginning. According to the scheme of the PSG classification, there are only two ways to realize the translational symmetry for a Z_2 spin liquid³¹. In the first class, the mean field ansatz should be manifestly translational invariant. In the second class, the unit cell of the mean field ansatz should be doubled and a Z_2 gauge transformation is needed to restore the translated ansatz. In this study we will concentrate on the second class since it is energetically much more favorable than the first class. It can also be shown that only the second kind of RVB state can be connected continuously to the U(1) Dirac spin liquid phase.

In our study, we will adopt a $L \times L \times 3$ cluster as illustrated in Fig.1. The doubled unit cell is illustrated by the region within the pink parallelogram. According to the PSG of the state, the RVB order parameters on the dashed bonds should be multiplied by an additional minus sign as compared to the RVB order parameters on the solid bonds translated from them. The on-site RVB order parameters should be manifestly translational invariant. As a result, we have 3 independent on-site RVB order parameters, 6 independent RVB order parameters on the NN bonds and 6 independent RVB order parameters on the NNN bonds. Using the remaining gauge degree of freedom allowed by the translational symmetry, we can transform the RVB order parameters on the gray sites and the RVB order parameters on the two NN bonds from the gray sites into the form of $\alpha\tau_3$. Finally, we can transform the pairing order parameter on a third NN bonds into real. Taking all these considerations into account, we are left with 48 independent real variational parameters.

We have performed large scale variational optimization on the above RVB ansatz for the $J_1 - J_2$ model on the kagome lattice. We have adopted the Stochastic Reconfiguration method in our variational search³². The optimized RVB ansatz is illustrated in Fig.1. More specifically, the on-site RVB order parameter are given by

$$U_{i,i} = \begin{cases} \mu\tau_3 & \text{gray sites} \\ \mu\vec{n}_{\phi_1} \cdot \vec{\tau} & \text{navy sites} \end{cases} \quad (4)$$

in which $\vec{\tau} = (\tau_1, \tau_2, \tau_3)$ are the Pauli matrixes, $\vec{n}_{\phi} = (\sin(\phi), 0, \cos(\phi))$ is a vector of unit length in the $\tau_1 - \tau_3$ plane. μ is a real number. The RVB order parameters on the nearest-neighboring(NN) bonds are given by

$$U_{i,j} = -s_{i,j} \begin{cases} \tau_3 & \text{black bonds} \\ \vec{n}_{\phi_2} \cdot \vec{\tau} & \text{red bonds} \end{cases} \quad (5)$$

Here $s_{i,j} = \pm 1$ on the solid(dashed) NN bonds. The RVB order parameter on the next-nearest-neighboring(NNN) bonds are given by

$$U_{i,j} = -\nu_{i,j} \begin{cases} \eta\vec{n}_{\phi_3} \cdot \vec{\tau} & \text{blue bonds} \\ \eta\vec{n}_{\phi_4} \cdot \vec{\tau} & \text{green bonds} \end{cases} \quad (6)$$

Here η is a real number, $\nu_{i,j} = \pm 1$ on the solid(dashed) NNN bonds.

The above ansatz is manifestly time reversal symmetric but may in general break the point group symmetry of the kagome lattice. However, we find at the optimum of the variational energy, the following relations always hold: $\phi_1 = 2\phi_2, \phi_4 = \phi_3 + \phi_2$. In such a situation, we can actually prove that the ansatz describes a fully symmetric spin liquid state. In fact, we can show that the above RVB ansatz is gauge equivalent to the Z_2 ansatz proposed

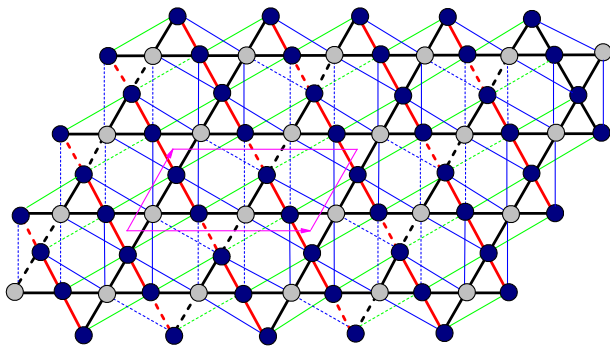


FIG. 1: The mean field ansatz of the Z_2 spin liquid state studied in this paper. The region within the pink parallelogram is the unit cell of the mean field Hamiltonian. The dots(bonds) in the same color have the same value for the RVB order parameter $U_{i,j}$, except for an additional minus sign on the dashed bonds.

in Ref.[1] by the following gauge transformation

$$G_i = \begin{cases} \exp(-i\frac{\phi_2\tau_2}{2}) & i \in \text{gray sites} \\ \exp(i\frac{\phi_2\tau_2}{2}) & i \in \text{navy sites} \end{cases} \quad (7)$$

The gauge transformed ansatz takes the form of

$$U_{i,j} = \begin{cases} \mu\vec{n}_{\phi_2} \cdot \vec{\tau} & \text{on-site} \\ -s_{i,j}\tau_3 & \text{NN bonds} \\ -\nu_{i,j}\eta\vec{n}_{\phi_3} \cdot \vec{\tau} & \text{NNN bonds} \end{cases} \quad (8)$$

When both ϕ_2 and η are set to be zero, the above ansatz is reduced to the U(1) Dirac spin liquid ansatz. To break the U(1) gauge symmetry, we can introduce a nonzero pairing term either on a site or on a NNN bond. More specifically, if there exists two closed loops starting from the same point, say, site i , on which the successive product of the RVB order parameters $P_i = U_{i,j}U_{j,k}\dots U_{l,i}$ do not commute, the U(1) gauge symmetry is broken. To determine the gauge structure of the above ansatz, we can define the following two closed loops. The first one is a length-zero loop consisting of the site i only. The product of RVB order parameters on this loop is just the on-site RVB order parameter $P_i^1 = U_{i,i} = \mu\vec{n}_{\phi_2} \cdot \vec{\tau}$. The second closed loop is the elementary triangle from site i . The product of RVB order parameters on this loop is given by $P_i^2 = U_{i,j}U_{j,k}U_{k,i} = -\tau_3$. Here i, j, k are the three vertices of the elementary triangle. Thus, the U(1) gauge symmetry is broken when $\phi_2 \neq 0$ or π . The deviation of ϕ_2 from 0 or π provides us a measure of the extent of the U(1) gauge symmetry breaking. For the above ansatz, the U(1) gauge symmetry is broken when $\phi_2 \neq 0, \pi$ even in the absence of NNN RVB order

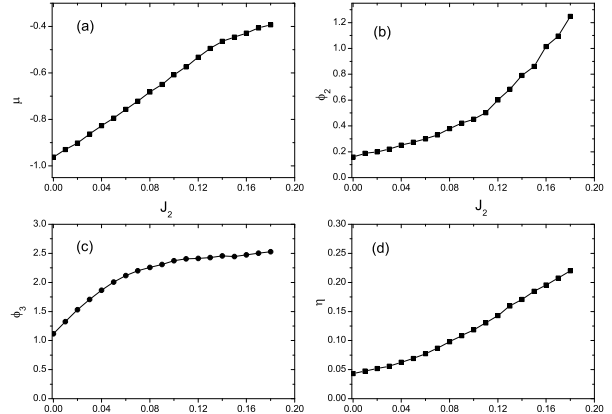


FIG. 2: The optimized variational parameters as a function of J_2 . The system size is $L = 12$ in the calculation

parameters. However, our numerical optimization shows that the NNN RVB order parameter is crucial to stabilize a Z_2 gauge structure. More specifically, if we set $\eta = 0$, then in the optimized ansatz we always have $\phi_2 = 0$. As we will see below, the optimized value of both ϕ_2 and η increase with J_2 . This is consistent with previous DMRG studies which find that the convergence of the topological entanglement entropy becomes better for larger J_2 .

Now we present our results of the variational calculation on the $J_1 - J_2$ model with the above RVB ansatz. Our calculation is done on a $L \times L \times 3$ cluster with L ranging from 12 to 24. We use periodic-anti-periodic boundary condition in all calculations. Previous studies on the same ansatz find that the U(1) Dirac spin liquid is the best variational state even for quite large J_2 on sufficiently large system. What we find here is different. We find the U(1) Dirac spin liquid is not the most stable state for both zero and non-zero J_2 on the largest system we have attempted, which is much larger than that is used in previous studies. In the fully symmetric state, there are four variational parameters, namely μ , ϕ_2 , ϕ_3 and η to be determined by optimization of the variational energy. In Fig.2 we plot the optimized values of the variational parameters as functions of J_2 ($J_1 = 1$). From the results, we see the extent of U(1) gauge symmetry breaking(which is dictated by the angle ϕ_2) increases monotonically with J_2 . At $J_2 = 0.15$, the breaking of the U(1) gauge symmetry is very significant.

To show that the Z_2 saddle point we find is indeed more stable than the U(1) saddle point found in previous studies, we plot the interpolation of the variational energy between these two saddle points. The U(1) saddle point is reached when we set $\phi_2 = 0$ and $\phi_3 = 0$. The value of η is in general nonzero for nonzero J_2 and should be optimized. We define an interpolation between the optimized U(1) ansatz and the optimized Z_2 saddle point

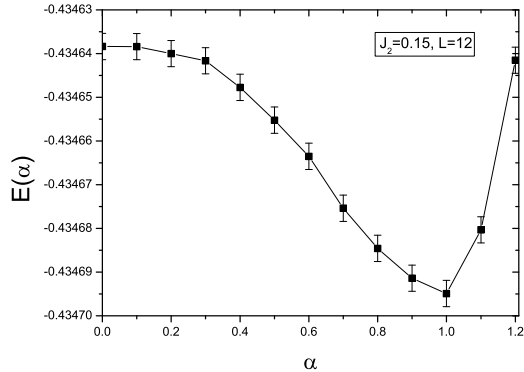


FIG. 3: The interpolation of the variational energy between the U(1) saddle point and the Z_2 saddle point. The calculation is done for $J_2 = 0.15$ on a $L = 12$ system.

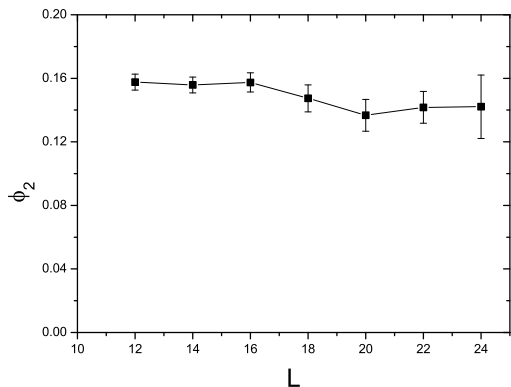


FIG. 4: The optimized value of ϕ_2 at $J_2 = 0$ for different system sizes.

by mixing their variational parameters in the following way: $x_i = \alpha x_i^{(0)} + (1 - \alpha)x_i^{(1)}$. Here α is an interpolation parameter, $x_i^{(0)}$ and $x_i^{(1)}$ denote the set of optimized variational parameters $(\mu, \phi_2, \phi_3, \eta)$ for the U(1) and Z_2 saddle point. The variational energy as a function of the interpolation parameter α at $J_2 = 0.15$ is shown in Fig.3. The Z_2 saddle point is obviously more robust than the U(1) saddle point. However, the energy difference between the two saddle points is extremely small (or the order of $10^{-4}J_1$ per site). This is very unusual since the difference in the gauge structure of the two saddle points is so significant.

At the same time, we find the Z_2 phase angle ϕ_2 remains nonzero even for $J_2 = 0$ (note the optimized value for η is significantly larger than previous report, which is $0.0186(2)^{28}$). To check if this is a finite size effect, we have performed the variational optimization on larger

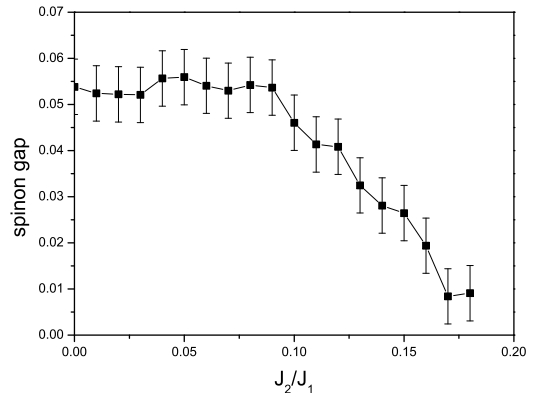


FIG. 5: The mean field spinon gap in the thermodynamic limit calculated with the optimized RVB parameters obtained on the $L = 12$ cluster.

systems. Fig.4 shows the size dependence of ϕ_2 up to $L = 24$, which is the largest size that we can deal with. We find although there is a tendency in ϕ_2 to decrease with increasing L , the slope is very small and it is hard to conclude if it vanishes on any finite system that we can treat. We note the largest L we have treated is already significantly larger than the circumference of the cylindrical clusters used in DMRG calculations. Thus it is possible that the weak signature of Z_2 spin liquid claimed by DMRG simulations at $J_2 = 0$ is still a finite size effect. The true ground state at $J_2 = 0$ in the thermodynamic limit may still be very close to a gapless U(1) spin liquid, or a quantum critical point³³.

Now let's investigate the evolution of the spin gap with J_2 . Usually, the spin gap opens when the mean field ansatz breaks the U(1) gauge symmetry. We thus should expect the spin gap to increase with the extent of U(1) gauge symmetry breaking. However, we find this is not true for our state. In principle, it is impossible to extract the spin gap directly from the variational calculation on the ground state. The spin correlation length in the ground state is also not a good indicator for the spin excitation gap for the kagome antiferromagnet. Here we will use the mean field result for the spinon gap as an indicator of the spin excitation gap. The evolution of the mean field spinon gap with J_2 is shown in Fig.5 (note the magnitude of the NN RVB order parameter has been set to be one). To reduce finite size effect, we have calculated the mean field dispersion in the thermodynamic limit with the optimized RVB parameters obtained on the $L = 12$ cluster. We find the spinon gap actually decreases with increasing J_2 and approaches zero around $J_2 = 0.2$, a signature which may imply the proximity of the system to a magnetic ordered state at large J_2 ²⁴.

Finally, let us return to the problem of the exceptional insensitivity of the variational energy in the RVB parameters as we find in Fig.3. Similar behavior has also been

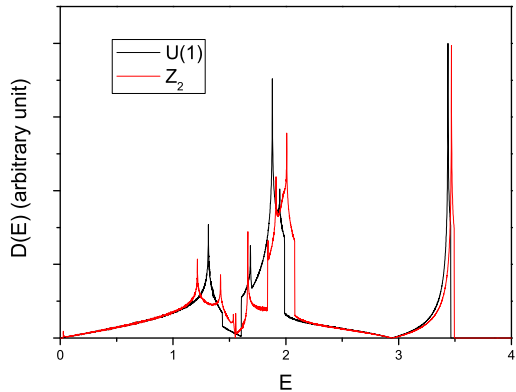


FIG. 6: The density of state of the U(1) and Z_2 ansatz at $J_2 = 0.15$.

reported in previous variational studies of the kagome antiferromagnet. A possible origin for such a strange behavior is that the saddle points with distinct RVB parameters may correspond to similar spin liquid state. This implies that some RVB parameters may be quasi-redundant. To check if this is the case, we have calculated the overlap between the U(1) spin liquid state and the Z_2 spin liquid state at $J_2 = 0.15$. To our surprise, we find the overlap is larger than 0.99 on the $L = 12$ cluster (the overlap at J_2 is even larger). To find out the origin for such a quasi-redundancy, we plot in Fig.6 the density of state of spinon excitation for the two ansatzs at $J_2 = 0.15$. Except for the small gap feature around $E = 0.03$ for the Z_2 ansatz, the density of state of both ansatzs are almost identical below $E = 1$. The density of state for both states become drastically different

only when $E > 1$. This implies that the main difference between the two states is in their high energy behavior, which for some reason depend only very weakly on the structure of the ground state. This is possible for a multi-band system, in which totally different high energy excitation spectrum can be realized on the same ground state. It is interesting to see if similar behavior also occurs for RVB states on other on-primitive Bravais lattices.

In summary, we have performed large scale search for Z_2 spin liquid state for the spin- $\frac{1}{2}$ kagome antiferromagnet with NN and NNN exchanges assuming only translational invariance. We find the best RVB state is always fully symmetric and is gauge equivalent to a Z_2 ansatz proposed previously from symmetry analysis. The Z_2 state is found to be slightly more stable than the extensively studied U(1) gapless Dirac spin liquid state in both the $J_2 \neq 0$ and the $J_2 = 0$ case and to possess a small spinon gap for $J_2 < 0.2$. We find while the extent of U(1) gauge symmetry breaking in the Z_2 state increases with J_2 , the spinon gap follows the opposite trend. These results are qualitatively consistent with the findings of the DMRG simulations on the $J_1 - J_2$ model on the kagome lattice. However, we note the Z_2 state we find is always very close to the gapless U(1) Dirac spin liquid state, although they have very different RVB parameters. Thus we think the kagome antiferromagnet should be better understood as a near critical system, rather than a system deep inside a gapped spin liquid phase with well established Z_2 topological order.

This work is supported by NSFC Grant No. 11034012 and the Research Funds of Renmin University of China. The author acknowledge the discussion with Tomonori Shirakawa, Seiji Yunoki, Yuan-Ming Lu, Normand Bruce and Fa Wang in different stages of this work.

-
- ¹ V. Elser, Phys. Rev. Lett. **62**, 2405 (1989).
² J. T. Chalker and J. F. Eastmond, Phys. Rev. B **46**, 14201 (1992).
³ P. W. Leung and V. Elser, Phys. Rev. B **47**, 5459 (1993).
⁴ N. Elstner and A. P. Young, Phys. Rev. B **50**, 6871 (1994).
⁵ P. Lecheminant, B. Bernu, C. Lhuillier, L. Pierre, and P. Sindzingre, Phys.Rev.B **56**, 2521 (1997).
⁶ P. Sindzingre and C. Lhuillier, Europhys. Lett. **88**, 27009 (2009).
⁷ H. Nakano and T. Sakai, J. Phys. Soc. Jpn. **80**, 053704 (2011).
⁸ A. M. Läuchli, J. Sudan, and E. S. Sørensen, Phys. Rev. B **83**, 212401 (2011).
⁹ R. R. P. Singh and D. A. Huse, Phys. Rev. Lett. **68**, 1766 (1992); R. R. P. Singh and D. A. Huse, Phys. Rev. B **76**, 180407(R) (2007); R. R. P. Singh and D. A. Huse, Phys. Rev. B **77**, 144415 (2008).
¹⁰ G. Evenbly and G. Vidal, Phys. Rev. Lett. **104**, 187203 (2010).
¹¹ C. Waldtmann, H.-U. Everts, B. Bernu, C. Lhuillier, P. Sindzingre, P. Lecheminant, and L. Pierre, Eur. Phys. J. B **2**, 501 (1998); P. Sindzingre, G. Misguich, C. Lhuillier, B. Bernu, L. Pierre, Ch. Waldtmann, and H.-U. Everts, Phys. Rev. Lett. **84**, 2953 (2000); G. Misguich and B. Bernu, Phys. Rev. B, **71**, 014417(2005); A. M. Läuchli and C. Lhuillier, arXiv:0901.1065.
¹² F. Mila, Phys. Rev. Lett. **81**, 2356(1998); M. Mambrini and F. Mila, Eur. Phys. J. B **17**, 651 (2000).
¹³ R. Budnik and A. Auerbach, Phys. Rev. Lett. **93**, 187205 (2004).
¹⁴ D. Poilblanc, M. Mambrini, and D. Schwandt, Phys. Rev. B **81**, 180402 (2010).
¹⁵ J. S. Helton, K. Matan, M. P. Shores, E. A. Nytko, B. M. Bartlett, Y. Yoshida, Y. Takano, A. Suslov, Y. Qiu, J.-H. Chung, D. G. Nocera, and Y. S. Lee, Phys. Rev. Lett. **98**, 107204 (2007).
¹⁶ P. Mendels, F. Bert, M. A. de Vries, A. Olariu, A. Harrison, F. Duc, J. C. Trombe, J. S. Lord, A. Amato, and C. Baines,

- Phys. Rev. Lett. **98**, 077204 (2007).
- ¹⁷ T. H. Han, J. S. Helton, S. Chu, D. G. Nocera, J. A. Rodriguez-Rivera, C. Broholm, Y. S. Lee Nature **492**, 406410 (2012).
- ¹⁸ H. C. Jiang, Z. Y. Weng, and D. N. Sheng, Phys. Rev. Lett. **101**, 117203 (2008).
- ¹⁹ S. Yan, D. A. Huse, and S. R. White, Science **332**, 1173 (2011).
- ²⁰ S. Depenbrock, I. P. McCulloch, and U. Schollwöck, Phys. Rev. Lett. **109**, 067201 (2012).
- ²¹ H. C. Jiang, Z. Wang, and L. Balents, Nat. Phys. **8**, 902 (2012).
- ²² S. S. Gong, W. Zhu, and D. N. Sheng, Sci. Rep. **4**, 6317 (2014).
- ²³ F. Kolley, S. Depenbrock, I. P. McCulloch, U. Schollwöck, V. Alba, Phys. Rev. B **91**, 104418 (2015).
- ²⁴ S. S. Gong, W. Zhu, L. Balents, and D. N. Sheng, Phys. Rev. B **91**, 075112 (2015).
- ²⁵ M. B. Hastings, Phys. Rev. B **63**, 014413 (2000).
- ²⁶ Y. Ran, M. Hermele, P. A. Lee, and X. G. Wen, Phys. Rev. Lett. **98**, 117205 (2007).
- ²⁷ Y. M. Lu, Y. Ran, and P. A. Lee, Phys. Rev. B **83**, 224413 (2011).
- ²⁸ Y. Iqbal, F. Becca, and D. Poilblanc, Phys. Rev. B **83**, 100404(R) (2011).
- ²⁹ Y. Iqbal, F. Becca, and D. Poilblanc, Phys. Rev. B **84**, 020407(R) (2011); New J. Phys. **14**, 115031 (2012); Y. Iqbal, F. Becca, S. Sorella, and D. Poilblanc, Phys. Rev. B **87**, 060405(R) (2013); Y. Iqbal, D. Poilblanc, and F. Becca, Phys. Rev. B **89**, 020407(R) (2014).
- ³⁰ Y. Iqbal, D. Poilblanc, and F. Becca, Phys. Rev. B **91**, 020402(R) (2015).
- ³¹ X. G. Wen, Phys. Rev. B **65** 165113 (2002).
- ³² S. Yunoki and S. Sorella, Phys. Rev. B **74**, 014408 (2006).
- ³³ Tao Li, arXiv:1106.6134.